

Change in the interfacial reaction of Hf-silicate film as a function of thickness and stoichiometry

M.-H. Cho,^{1,a)} C. Y. Kim,¹ K. Moon,¹ K. B. Chung,² C. J. Yim,³ D.-H. Ko,³ H. C. Sohn,³ and Hyeongtag Jeon⁴

¹*Institute of Physics and Applied Physics, Yonsei University, Seoul 120-749, South Korea*

²*Department of Physics, North Carolina State University, Raleigh, North Carolina 27695-8202 USA*

³*Department of Material Science and Engineering, Yonsei University, Seoul 120-749, South Korea*

⁴*Department of Material Science and Engineering, Hanyang University, Seoul 133-791, South Korea*

(Received 6 February 2008; accepted 10 June 2008; published online 18 July 2008)

Medium energy ion scattering and high-resolution transmission electron microscopy are used to investigate the depth of the interfacial reaction of Hf-silicate film. The interfacial reaction is critically affected by the film thickness and the mole fraction of HfO₂ in silicate film. The interfacial compressive strain generated at the surface of the Si substrate is dependent on the film thickness during the postannealing process in film with a thickness of ~4 nm. Finally, the phase separation phenomenon demonstrates critically different behaviors at different film thicknesses and stoichiometries because the diffusion of Si from interface to surface is dependent on these factors. Moreover, the oxidation by oxygen impurity in the inert ambient causes SiO₂ top formation. © 2008 American Institute of Physics. [DOI: 10.1063/1.2955461]

Hf-based high-dielectric oxides are the leading candidates for replacement of SiO₂/SiON as the gate dielectric of choice in complementary metal-oxide-semiconductor (CMOS) devices for nodes beyond 45 nm. Particular attention has recently been given to (HfO₂)_x(SiO₂)_{1-x} films that demonstrate a variety of attractive properties for alternate gate dielectric applications, such as a relatively high-dielectric constant, thermal stability that is better than HfO₂, and no interdiffusion with the Si substrate.¹⁻³

However, some studies have recently predicted that there are two limiting mechanisms by which phase-separated microstructures in Hf- and Zr-silicate films evolve, depending on the film composition and annealing temperature. The observed metastable miscibility gap causes an amorphous film to lower its free energy by separating into two phases with compositions. Recently, Kim *et al.* reported that spinodal decomposition can occur through diffusional phase separation. This finding was confirmed for a ZrO₂-SiO₂ system.⁴ Neumayer *et al.* showed that phase separation and crystallization occur after annealing at a temperature of 800 °C in HfO₂-SiO₂ systems with HfO₂ concentrations higher than 50% and less than 25% at 1000 °C.⁵ Moreover, in practice, the phase separation of binary mixtures often proceeds under the presence of an external field. In particular, in ultrathin film the interfacial effect can critically affect the phase separation kinetics.⁶

Our group noted that these studies are based on metastable phase diagrams in thin film with a specific thickness. Some studies have reported that the temperature for phase separation is changed by the thickness and stoichiometry of the silicate films.⁶⁻⁹ However, these studies have not considered the interfacial reactions between the film and the Si

substrate during phase separation, although reactions in thin films with a thickness in the approximately nanometer range can critically affect the phase separation phenomenon, depending on the HfO₂ and SiO₂ contents in the silicate film.

In this study, our group experimentally showed that the interfacial reaction is closely related to the film thickness and stoichiometry in HfO₂-SiO₂ binary oxide mixtures, which affect the diffusional phase separation in a depth direction. The diffusion process is critically influenced by the interfacial reaction, which is caused by the relaxation process of the interfacial strain. At a critical film thickness, phase separation occurs vertically during the postannealing process, while vertical separation is not observed in a relatively thick film.

The metal oxides used in this study were grown using an atomic layer deposition (ALD) system, which has a vertical warm-wall reactor with a showerhead and a heated susceptor. SiO₂ and HfO₂ films were grown at temperatures below 280 °C using tris(dimethylamido)silane (tDMAS) and tetrakis(ethylmethylamido) hafnium (TEMAH), respectively, as precursors. O₃ vapor [flow rate=450 SCCM (SCCM denotes cubic centimeter per minute at STP)] served as the oxygen source, and N₂ (flow rate=450 SCCM) was supplied as the purge and carrier gas. The SiO₂-incorporated Hf-Si-O were grown by the alternate ALD process, repeating the number of cycles for HfO₂ and SiO₂ to mix the SiO₂ content in a controlled manner. The ALD process deposited 2-nm-7-nm-thick (HfO₂)_x(SiO₂)_{1-x} films on Si with two different compositions: 25 mol % HfO₂-75 mol % SiO₂ ($x=0.25$) and 65 mol % HfO₂-35 mol % SiO₂ ($x=0.65$). The films were annealed using a rapid thermal process system in a N₂ ambient atmosphere at a temperature of from 800 to 900 °C.

The stoichiometry and strain in the depth direction was assessed by medium-energy ion scattering (MEIS) using a H⁺ beam with an incident energy of 100 keV. The data pro-

^{a)}Electronic mail: mh.cho@yonsei.ac.kr.

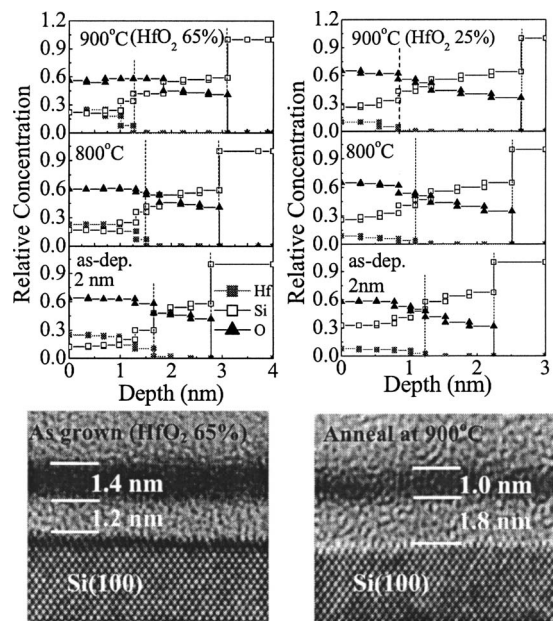


FIG. 1. Concentration in the depth direction of the 2-nm-thick HfSiO film (1.4 nm thickness in HRTEM image) with the mole fractions of HfO₂ ($x=0.25, 0.65$) is calculated from the MEIS spectra. The change in the concentration after annealing treatment at 800 and 900 °C is also obtained. No crystallization and increment of the interfacial layer are observed in the HRTEM image of HfSiO even with HfO₂ fraction of 65%.

vided critical proof that the diffusion of Si from the substrate was generated, resulting in a phase separation that started at the surface with SiO₂ extraction. The change in the blocking dip also showed that a strain was generated at the interface, which was dependent on the film thickness and the quantity of SiO₂ in the film. After the thermal annealing process, the relaxation of interfacial strain and the behavior of phase separation were also dependent on the film thickness. Phase separation in a depth direction was confirmed by high-resolution transmission electron microscopy (HRTEM). A MEIS analysis was conducted in a double-alignment mode to reduce contributions from the crystalline Si substrate, allowing the deconvolution of the spectra into contributions from the SiO₂ layer and Si signals. The incident ions were located along the (111) plane, and the scattered ions were located along the (001) plane with a scattering angle of 125° in order to obtain quantitative depth profiles. The blocking dips around the $\langle 111 \rangle$ direction in the (110) plane were measured in a single alignment to improve counting statistics. The angular resolution, determined mainly by an incident ion beam divergence and a position sensitive detector, was estimated at an angle better than 0.1°.¹⁰

Figure 1 shows an atomic image of the films with a calculated concentration of 2-nm-thick Hf-silicate films with a high ($x=0.65$) and low HfO₂ mole fractions ($x=0.25$) using HRTEM and MEIS energy spectra, respectively. In particular, our group did not observe any crystallization in the HRTEM image of the films with high HfO₂ content after an annealing treatment of as high as 900 °C, although the Hf-silicate layer shrank. Our group found stoichiometric change in the interfacial layer after the annealing treatment, which could have been caused by the interfacial reaction from residual oxygen during the annealing process. Moreover, the

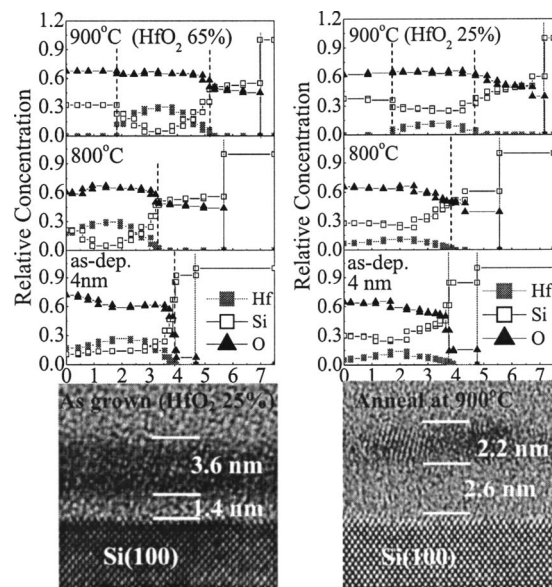


FIG. 2. Concentrations in the depth direction of the 4-nm-thick HfSiO film (3.6 nm thickness in HRTEM image) with the mole fractions of HfO₂ ($x=0.25, 0.65$) are calculated from the MEIS spectra. The MEIS data and HRTEM image show the significant increase in the interfacial layer and the shrinkage of the film after the annealing treatment at 900 °C.

concentration of SiO₂ in the film increased after the annealing treatment, as shown in the MEIS data. This indicated that Si was diffused from the interface to the film. These results showed, therefore, that a high content of SiO₂ in a very thin layer disturbed the crystallization of the silicate film.

The change in the quantity of Hf and Si can be more clearly observed in the thick (4 nm) Hf-silicate film, as shown in Fig. 2. The energy position and shape of the Hf peak at the leading edge in MEIS energy spectra showed that the stoichiometry at the surface region of the as-grown silicate film is changed through the extraction of SiO₂ from the film even after annealing at 800 °C. As the annealing temperature increased to 900 °C, the depth profile of the stoichiometry from the MEIS data indicated that a very thick interfacial SiO₂ layer was formed, resulting from a high interfacial reaction. Moreover, a thin SiO₂ layer, with a thickness of less than 2 nm, was completely segregated over the film surface. The quantity of extracted SiO₂ over the film surface exceeded the incorporated mole fraction of SiO₂ in the as-grown film. The diffused SiO₂ content contained in the silicate film was totally dependent on the mole fraction of SiO₂ in the as-grown film. The Hf peak change in width and intensity indicated that no movement of Hf occurred, confirming that Si generated at the interface between the film and the Si substrate had diffused to the film surface. The extraction of SiO₂ from the film and the diffusion of newly generated SiO₂ from the interface to the film surface were observed in all samples, although the extraction quantity was dependent on the level of SiO₂. This result is not consistent with the theoretically predicted data, which show that phase separation begins at the interface because of a large local gradient in SiO₂ chemical potential.⁴ Our group's data showed that the phase separation begins at the surface. Comparing the interfacial layer thickness with that of a 2-nm-film thickness, the interfacial layer was significantly increased in

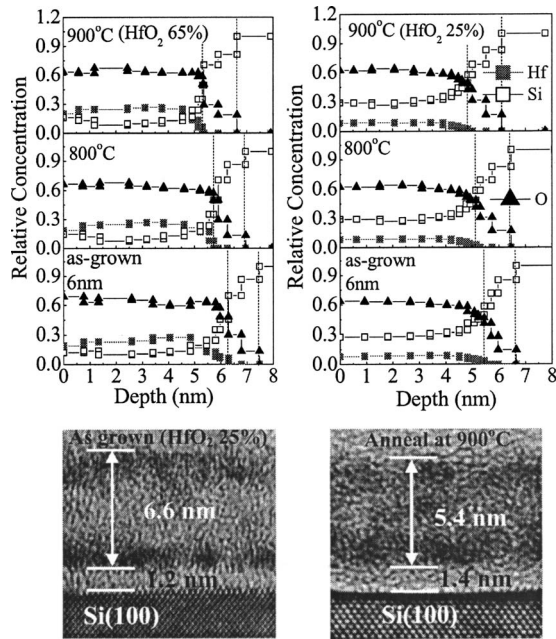


FIG. 3. Change in the concentration of the 7-nm-thick HfSiO (6.6 nm thickness in HRTEM image) with the 65% and 25% fractions of HfO₂ are obtained using MEIS energy spectra. Change in the interfacial layer is slightly occurred as the annealing temperature increases, while shrinkage of the film is observed as shown in the 2-nm- and 4-nm-thick films. The HRTEM image shows random local phase separation after the annealing treatment at 900 °C.

a 4-nm-thick silicate film. Thus, the interfacial reaction can be related to the diffused quantity of SiO₂ from the interfacial region to the film surface, which affected the phase separation phenomena in a depth direction. The crystallization of the film with high SiO₂ content ($x=0.25$) was localized, indicating that the phase separation occurred dominantly through spinodal decomposition. Thus, the high quantity of SiO₂ content diffused from the interface to the film can contribute to the dominant spinodal decomposition.

The tendency of the interfacial reaction and the diffusion of Si from the interface with a relatively thick film (7 nm) are shown in Fig. 3. Any significant change in stoichiometry in the depth direction of the 7-nm-thick Hf-silicate film was not observed even in different HfO₂ mole fractions, i.e., the minute increase in the SiO₂ content at the film surface was observed only in the film with a high HfO₂ fraction. The HRTEM image also supports the lack of change in stoichiometry in the depth direction. Of more importance to the MEIS spectra and the TEM image is the fact that the formation of a thick interfacial layer and crystallization were not observed during the annealing treatment with temperatures as high as 900 °C, compared with the changes in the 4-nm-thick film. Thus, the interfacial reaction in the 7-nm-thick films is more suppressed than that with 4-nm-thick films. The oxidation after postannealing treatment indicates that the formation of the top SiO₂ layer is caused by the oxidation process at the interface. The oxygen impurity contained in the inert ambient conditions during the oxidation process causes the interfacial oxidation, resulting in the top SiO₂ formation through the diffusion of Si from the interface of SiO₂/Si. The difference in the interfacial

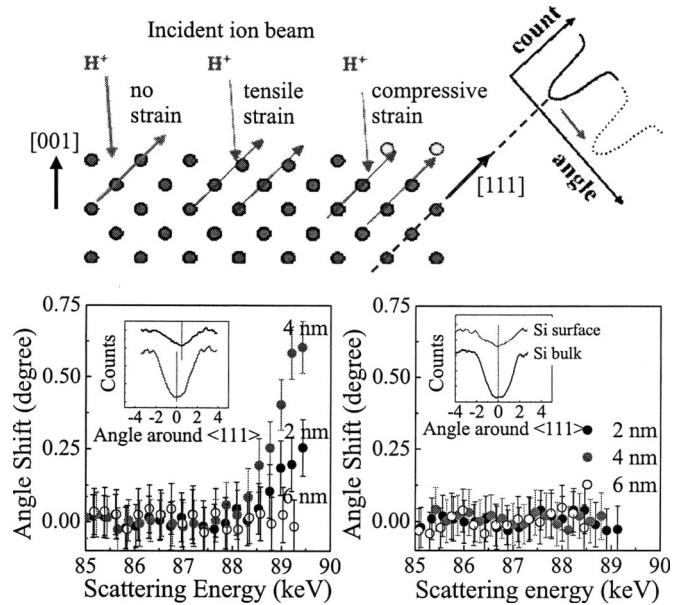


FIG. 4. The schematic diagram of measurement of blocking dip using MEIS: the direction of incident and scattered beam and atomic arrangement is described. The angular shift of the Si blocking dip from the Si substrate is dependent on the film thickness (left side). The angular shift is also obtained from the films after the annealing treatment at 900 °C (right side). The inset is the blocking dips of Si bulk and Si surface contacting the film. After the annealing treatment, the shift of the blocking on Si surface is not observed.

layer thickness after postannealing treatment strongly suggests that the diffusion of Si from the interface of SiO₂/Si is related to the relaxation of stress that is induced by oxidation.^{11,12} Thus, accumulated stress, which is inevitable in Si oxidation, can be a main factor of Si diffusion. Moreover, our data showed that interfacial stress is related to the phase separation of the film because the effect is dependent on the stoichiometry and the thickness of the films.

The stoichiometric change in the depth direction attributed to diffusion indicates that the high interfacial strain can be a main factor in changing the atomic transportation because the evolution of strain in the depth direction can easily change the stoichiometry in the depth direction.¹³ To investigate the cause of the interfacial reaction resulting in the diffusion of Si from the interface, our group investigated the stress change in different thicknesses of films using MEIS, as shown in Fig. 4. The scattered ion beam in a specific direction (in this experiment, the direction is [111]) is blocked at the surface atoms, resulting in blocking dips. Thus, the position of the blocking dip reflects the position of atoms at the direction. This also revealed short-range information such as the elastic strain and the registry of the overlayer. As shown in Fig. 4, if there is no strain at the interface, the atomic arrangement at the interface is not changed. When the interfacial strain is applied to the interfacial region, the atomic position is changed at the interface; i.e., a different strain direction can be measured by the change in the blocking dip position. Moreover, the change in the atomic position in the depth directions can be detected using an electrostatic energy analyzer. The strain distribution was analyzed through changes in the blocking dips at various energies that corresponded to the depth of the Si surface under the film. Figure

4 shows the angular shift of the Si blocking as a function of the scattering energy in investigating the strain distribution in depth direction. Although the angular position agrees with the bulk [111] axis at deeper regions, the dip shifts toward larger incident angles when approaching the interface. The local compressive strain at the top surface of the Si can be estimated from the observed angular shift $\Delta\theta$ by $\varepsilon = 2\Delta\theta/\sin 2\theta$. The observed strain was about 1% at the 2-nm-thick Hf-silicate film interface, and it rapidly increased over 2.2% at the 4-nm-thick film interface. The distribution of the strain indicates that the maximum compressive strain is located at the top surface of the Si that contacts the film; the blocking dip is shifted to a higher angle at the interface. This was because the high stress at the amorphous film transfers to the substrate, resulting in a regular change in the ordering of the Si atoms at the surface of the Si substrate. The maximized tetragonal distortion of the Si atom at the Si surface gradually decreased to expand beneath the surface. The strain value is very high compared to that of the strained Si film for mobility enhancement in CMOS technology; the reported compressive strain is less than 1%.^{14,15} Moreover, the strain in the metal-oxide-semiconductor field effect transistor device is enhanced because the lateral strained region is limited in the device size. However, in infinite films such as our samples, the high strain implies the presence of defects: i.e., the deep blocking dips in the bulk Si changes to shallow dips in the transition layer, as shown in the inset of Fig. 4, which means that the crystallinity in the transition layer is smaller than in the substrate crystalline Si. In the MEIS data, we find that the strain in the transition layer of the Si surface is gradually increased in the direction of the Si surface and the maximum value is localized at the thinner surface region. Thus, the high strain can be generated because of this gradual change in the strain in the transition region. This study's most important finding is that the shift of the angular position caused by local strain is critically dependent on the film thickness, i.e., in the 4-nm-thick silicate film, the strain is relatively high compared with that in the 2-nm-thick film. The angle shift indicates that the Si lattice in the as-grown films is compressed in the in-plane direction around the interface region, although the compressed lattice is completely relaxed after the annealing treatment at 900 °C. Consequently, these strain distributions and their relaxation indicate that the formation of the interfacial layer and the diffusion of SiO₂ in the depth direction can be related to the strain changes because the diffusion of SiO₂ can be caused by the interfacial strain through the strain relaxation process. Thus, when a relatively small strain is generated in thin film of 2 nm, the change in the interfacial layer and Si quantity at the film surface caused by Si diffusion occurs slightly. In the case of the 4-nm-thick film with very high strain, the occurrence of the formation of the interfacial layer and the diffusion of the Si atom from the interface is

significant. However, it is peculiar that the film with 7 nm thickness contained no strain in the depth direction. There also was no difference in strain between the as-grown film and the annealed film. No change in the Si content in the depth direction of the 7-nm-thick silicate film, even after the annealing treatment (as shown in the MEIS energy spectra of Figure 4), can provide the relationship of interfacial reaction with interfacial strain. Previous studies of the highly non-ideal mixing thermodynamics of the binary system with a high molar volume difference suggest that internal strain will develop in the amorphous films.^{4,7} Thus, phase separation in the binary systems can be influenced by the effects of local stress.

In conclusion, the interfacial reaction and diffusion of SiO₂ from the interface to the surface is dependent on the film thickness of the Hf-silicate film. The generated strain is dependent on the film thickness, resulting in the differing phase separation phenomenon during the relaxation of the accumulated strain. Moreover, interfacial oxidation by oxygen impurities in inert ambient conditions results in the diffusion of Si from the interface to the surface after the post-annealing process, which causes the SiO₂ top formation.

This work was partially supported by the National Program for Tera-level Nanodevices of the Ministry of Science and Technology as one of the 21st Century Frontier Programs. This work was supported by the Korean Research Foundation Grant funded by the Korean Government (MOE-HRD) (KRF-2007-357-C00020).

- ¹G. D. Wilk, R. M. Wallace, and J. M. Anthony, *J. Appl. Phys.* **87**, 484 (2000).
- ²G. Wilk, R. M. Wallace, and J. M. Anthony, *J. Appl. Phys.* **89**, 5243 (2001).
- ³G. Lucovsky, G. B. Rayner, and R. S. Johnson, *Microelectron. Reliab.* **41**, 937 (2001).
- ⁴H. Kim and P. C. McIntyre, *J. Appl. Phys.* **92**, 5094 (2002).
- ⁵D. A. Neumayer and E. Cartier, *J. Appl. Phys.* **90**, 1801 (2001).
- ⁶P. Koblinski, S. Kumar, A. Martian, J. Koplik, and J. R. Banavar, *J. Appl. Phys.* **76**, 1106 (1996).
- ⁷S. Stemmer, Y. Li, B. Foran, P. S. Lysaght, S. K. Streiffer, P. Fuoss, and S. Seifert, *Appl. Phys. Lett.* **83**, 3141 (2003).
- ⁸M.-H. Cho, K. B. Chung, C. N. Whang, D. W. Lee, and D.-H. Ko, *Appl. Phys. Lett.* **87**, 242906 (2005).
- ⁹M. A. Quevedo-Lopez, J. J. Chambers, M. R. Visokay, A. Shanware, and L. Colombo, *Appl. Phys. Lett.* **87**, 012902 (2005).
- ¹⁰Y. P. Kim, S. K. Choi, H. K. Kim, and D. W. Moon, *Appl. Phys. Lett.* **71**, 3504 (1997).
- ¹¹H. Kageshima and K. Shiraishi, *Phys. Rev. Lett.* **81**, 5936 (1998).
- ¹²Z. Ming, K. Nakajima, M. Suzuki, K. Kimura, M. Uematsu, K. Tori, S. Kamiyama, Y. Nara, and K. Yamada, *Appl. Phys. Lett.* **88**, 153516 (2006).
- ¹³D. Jalabert, J. Coraux, H. Renevier, B. Daudin, M.-H. Cho, K. B. Chung, D. W. Moon, J. M. Llorens, N. Garro, A. Cros, and A. Garcia-Cristobal, *Phys. Rev. B* **72**, 115301 (2005).
- ¹⁴K. Usuda, T. Numata, T. Irisawa, N. Hirashita, and S. Takagi, *Mater. Sci. Eng., B* **124-125**, 143 (2005).
- ¹⁵Y.-Y. Fang, J. Tolle, J. Tice, A. V. G. Chizmeshya, J. Kouvetakis, V. R. D'Costa, and J. Menendez, *Chem. Mater.* **19**, 5910 (2007).